

## Platinum Nanoparticles and Carbon Nanopolymer Composite as Sensor for Highly Sensitive Determination of Salbutamol in Pork Meat and Pork Liver

Jun-Yi He<sup>1,†</sup>, Xing Peng<sup>1,†</sup>, Pan-Pan Liang<sup>1</sup>, Wang Xiang<sup>1</sup>, Dan Li<sup>1,\*</sup>, Jing-Lei Xie<sup>1</sup>, Ling Wu<sup>1</sup>, Donghong Yu<sup>2,\*</sup>, Zhong Cao<sup>1,\*</sup>

<sup>1</sup> Hunan Provincial Key Laboratory of Materials Protection for Electric Power & Transportation and Hunan Provincial Key Laboratory of Cytochemistry, School of Chemistry and Chemical Engineering, Changsha University of Science and Technology, Changsha 410114, China

<sup>2</sup> Department of Chemistry and Bioscience, Aalborg University, DK-9220 Aalborg, East, Denmark

<sup>†</sup> These authors contributed equally to this work.

\*E-mail: [LD1004@126.com](mailto:LD1004@126.com), [yu@bio.aau.dk](mailto:yu@bio.aau.dk), [zhongcao2004@163.com](mailto:zhongcao2004@163.com)

Received: 7 November 2021 / Accepted: 27 November 2021 / Published: 5 January 2022

A metal-carbon nano-polymer based sensor was constructed by combining platinum nanoparticles (PtNPs), acidified multi-walled carbon nanotubes (MWCNTs), and a ionic polymer of perfluorinated sulfonic resin (PFSE) for modifying on the surface of glassy carbon electrode (GCE), yielding PtNPs/MWCNTs-PFSE/GCE. The behaviors of cyclic voltammetry (CV) and differential pulse voltammetry (DPV) of four different modified electrodes such as bare GCE, MWCNTs-PFSE/GCE, PtNPs/GCE and PtNPs/MWCNTs-PFSE/GCE were investigated in detail, showing that the PtNPs/MWCNTs-PFSE composite exhibited significantly improved electrocatalytic activity to salbutamol (SAL, **1**). An oxidation mechanism has been confirmed that the phenolic hydroxyl group of SAL (**1**) is oxidized involving one proton and one electron for a formation of a free radical, resulting in intermediate (**2**) via resonance, and then transform to a SAL dimmer (**3**) with a C-C bond formation via re-combination of the intermediate (**2**), showing an irreversible oxidation process. Under the optimum condition, the metal-carbon nano-polymer modified electrode showed excellent linear response to SAL in range of from  $5.0 \times 10^{-8}$  mol/L to  $2.0 \times 10^{-6}$  mol/L and a detection limit of  $1.4 \times 10^{-8}$  mol/L. The modified electrode possessed good selectivity, reproducibility, and stability. This has been successfully applied to determination of SAL content in pork meat and pork liver samples with recovery rates from 95.4% to 104.3%, indicating strong potential applications in food safety control.

**Keywords:** Salbutamol; Metal-carbon nano; Perfluorinated sulfonic resin; Pork meat and pork liver; Food safety

## 1. INTRODUCTION

As a synthetic  $\beta$ -adrenergic receptor agonist, salbutamol (SAL) is mainly used in clinics for the treatment of bronchial asthma, chronic pneumonia, and some respiratory allergy symptoms [1, 2]. On the other hand, SAL can promote the growth of animals, and transform the nutrients in animals from adipose tissue to muscle tissue. However, overdose or long-term intake of SAL in human body will lead to poisoning symptoms and even chromosomal malformations, malignant tumors, and other serious consequences [3, 4]. While SAL can easily remain in animal tissues and then enter human bodies through the food chain, it is of great importance to establish a quick and easy method for the detection of SAL.

Although currently many methods for SAL detection with good accuracy and sensitivity have been summarized as follows: spectrophotometry [5], fluorescence analysis [6,7], high performance liquid chromatography (HPLC) [8,9], liquid chromatography-mass spectrometry (LC-MS) [10-12], gas chromatography-mass spectrometry (GC-MS) [13,14], capillary electrophoresis (CE) [15], immunoassay [16-18], and surface-enhanced Raman spectroscopy [18], etc, they mostly required relatively expensive instruments, complex operation procedures, and long detection cycles, which cannot meet the need for real-time and rapid detection of large quantities of samples in practice, restricting the development of SAL detection technology to a certain extent.

On the contrary, electrochemical method has been more suitable for the detection of SAL on site, not only due to its advantages of high selectivity, high sensitivity, low cost and short detection cycles [19-27], but also based on the electroactive groups of SAL capable of being oxidized on the electrode surface [28]. Basically, there are three types of electrochemical sensors used for the detection of SAL. The first one is based on molecular imprinting method. Alizadeh *et al.* [29] reported a molecularly imprinted membrane based on Cu(II) for sensitive detection of SAL with a strong anti-interference ability based on the specifically selected membrane. But the membrane preparation was quite complicated, and it was difficult to use repeatedly [30]. The second type is based on immuno-reaction. Using Pd@SBA-15 labeled secondary antibody, a double anti-sandwich type of electrochemical immunosensor for detection of SAL with high sensitivity and selectivity was fabricated [31]. However, this type of sensor required preparation of high quality monoclonal antibodies with extremely harsh operation procedure and condition, which can not meet the rapid detection of large quantities of samples. The third type is based on catalyzing reactions. For example, Boyd *et al.* [32] investigated the electrochemical behavior of SAL on the electrode surface by using Nafion modified glassy carbon electrode, as an earlier report on catalytic electrochemical sensor for SAL. Goyal *et al.* [33] prepared gold nanoparticle modified indium tin oxide (NGITO) electrode for detection of SAL, followed by the adoption of multi-wall/single-wall carbon nanotubes modified electrodes for electrocatalytic detection of SAL [28,34,35]. Nevertheless, their low electron transfer rate based on such single component nanomaterial modified electrode limits the sensitivity of this type of sensor, it is therefore very necessary to establish more effective, sensitive, and stable SAL electrochemical sensors.

Meanwhile, precious metal nanoparticles/carbon nanotubes composites have recently attracted wide attention due to the unique properties for their uses as heterogeneous catalysis [36-40], fuel cell

[41], electrocatalysis, [42-47] and sensors [48-53] etc. At present, there are still very few reports on combining metal and carbon nanomaterials with ion polymer for electrochemical detections of SAL. Therefore, in this paper, in order to establish a SAL electrochemical sensor with high stability, high sensitivity, and strong anti-interference ability, a PtNPs/MWCNTs-polymer composite was successfully prepared by loading homogeneous and stable platinum nanoparticles into acidified multi-walled carbon nanotubes through liquid phase reduction method, and followed by dispersing in a perfluorinated sulfonic resin (PFSE) solution. The metal-carbon nano-polymer composite modified glassy carbon electrode (PtNPs/MWCNTs-PFSE/GCE) exhibited a strong electrocatalytic oxidation effect to SAL. And the oxidation mechanism has been deduced that the phenolic hydroxyl group of SAL (1) was oxidized involving one proton and one electronic for a formation of a free radical, followed by forming intermediate (2) via resonance, and then transformed into a SAL dimmer (3) with a C-C bond formation via re-combination of intermediate (2). The process was irreversible and had been confirmed by the electrochemical cyclic voltammetric studies. Such PtNPs/MWCNTs-PFSE/GCE can be used for the detection of SAL in ternary hybrid pig pork and pig liver samples with a recovery rate from 94.8% to 104.6%, which indicates a strong application in food safety.

## 2. EXPERIMENT

### 2.1 Reagents and Instruments

Salbutamol ( $C_{13}H_{21}NO_3$ , SAL) was obtained from Dr. Ehrenstorfer GmbH (Germany). Multi-walled carbon nanotubes (MWCNTs) were ordered from Jicang Nano Co. Ltd. (Nanjing, China). Perfluorinated sulfonic resin (PFSE) solution (20%, ethanol/water=2:1) was commercially purchased from Sigma-Aldrich Co. LLC (Merck, Germany). Chloroplatinic acid ( $H_2PtCl_6$ ), disodium hydrogen phosphate, sodium dihydrogen phosphate, uric acid, urea, ascorbic acid, glucose, glycine, L-leucine, L-arginine, L-cysteine, and L-tyrosine were all provided by Sinopharm Group Chemical Reagent Co. Ltd. (Shanghai, China). Phosphate-buffered saline (PBS) containing 0.01 mol/L  $Na_2HPO_4$ - $NaH_2PO_4$  was adopted for electrochemical detections. Ultra pure water with its electrical conductivity of  $\geq 18.3$  M $\Omega$ ·cm was prepared by a CZ-500L-W ultra-pure water device (Guozhiyuan Co. Ltd, Beijing, China). All reagents used in the experiment were of analytical grade.

All electrochemical experiments were performed on CHI760B electrochemical workstation (Shanghai Chenhua Instrument Co., Ltd., China), using a three-electrode system: PtNPs/MWCNTs-PFSE modified glassy carbon electrode (GCE) as a working electrode, a platinum wire electrode as a counter electrode, and an Ag/AgCl electrode (saturated KCl) as a reference electrode. Composite materials on electrode surface were characterized by JSM-6700 scanning electron microscopy (SEM, Japan Electronics Co. Ltd, Tokyo).

## 2.2 Preparation of PtNPs/MWCNTs Composites

Multi-walled carbon nanotube (100 mg) was added into a round bottom flask containing 75 mL of concentrated  $\text{HNO}_3$  solution. After heating and stirring for 7 h through oil bath, the mixture was cooled to room temperature and centrifuged for the removal of the supernatant. The resulted product was added into 50 mL concentrated  $\text{HCl}$ , centrifuged for 1 h to remove the supernatant, and washed with deionized water to neutralize the product. Vacuum drying at  $100\text{ }^\circ\text{C}$  for 10 h yielded the acidified multi-walled carbon nanotubes. 60 mg of such products were mixed with 20 mL of ultrapure water and 2 mL of  $0.0386\text{ mol/L}$   $\text{H}_2\text{PtCl}_6$  solution, ultrasonically shocked for 30 min, then placed in  $70\text{ }^\circ\text{C}$  water bath and stirred for 30 min. Next, 10 mL of a mixed solution of paraformaldehyde and  $\text{Na}_2\text{CO}_3$  was slowly added and then refluxed for 2.5 h, the resultant product was filtered to obtain a black solid. The black solids were washed with ultrapure water to neutral and vacuum dried at  $85\text{ }^\circ\text{C}$  for 10 h, thus, the nanocomposites were obtained.

## 2.3 Preparation of PtNPs/MWCNTs-PFSE/GCE

The above-attained black solid of 10 mg was added into 10 mL of PFSE-ethanol/water solution, ultrasonically shaken for 30 min, a dark gray uniform liquid was obtained as PtNPs/MWCNTs-PFSE composite dispersion.  $5\text{ }\mu\text{L}$  of these dispersion was taken and deposited onto the surface of a polished glassy carbon electrode for achieving PtNPs/MWCNTs-PFSE/GCE.

## 2.4 Electrochemical Detection of Salbutamol

In a PBS buffer ( $\text{pH}=2.5$ ), the PtNPs/MWCNTs-PFSE modified electrode was used as a working electrode with the platinum wire as a counter electrode and the  $\text{Ag/AgCl}$  electrode as a reference electrode to form the three-electrode system. Different concentrations of SAL solutions ( $5.0\times 10^{-8}$ ,  $1.0\times 10^{-7}$ ,  $2.0\times 10^{-7}$ ,  $5.0\times 10^{-7}$ ,  $1.0\times 10^{-6}$ ,  $1.5\times 10^{-6}$ , and  $2.0\times 10^{-6}\text{ mol/L}$ ) were tested by using differential pulse voltammetry (DPV), whereas the oxidation peak currents were recorded. Prior to the detection, the modified electrode was placed in PBS buffer for scanning to acquire a steady state in the range of 0 to 1.2 V.

## 2.5 Pretreatment of Actual Samples

Six ternary hybrid piglets weighed 7 Kg to 15 Kg and aged 30 months, were fed and provided by Institute of Subtropical Agriculture, Chinese Academy of Sciences (China), dividing into 6 groups. Each sample of 10 g of pork meat or pork liver was pretreated by firstly adding 20 mL  $0.1\text{ mol/L}$   $\text{HClO}_4$  solution to form homogenate, which was then ultrasonically shocked for 20 min, heated in  $80\text{ }^\circ\text{C}$  water bath for 30 min, and centrifuged for 15 min under the condition of 4500 r/min after cooling with supernatant obtained. The remaining precipitates were centrifuged again as described above. The combined supernatants were mixed with their pH adjusted to 10 with  $1.0\text{ mol/L}$   $\text{NaOH}$ .

solution, then the mixture was centrifuged again for 10 min. The resultant supernatant was transferred to a ground glass tube, added with 8 g of NaCl and 20 mL of isopropanol/ethyl acetate mixture with a volume ratio of 2:3, the upper organic phase was taken after being extracted for 20 min and centrifuged, then concentrated into solids in a water bath at 60 °C. The obtained solids were dissolved in 0.01 mol/L PBS (pH = 2.5) solution in a certain proportion for future use.

### 3. RESULTS AND DISCUSSION

#### 3.1 Characterization of Sensing Interface

The surface morphology of PtNPs-PFSE/GCE and PtNPs/MWCNTs-PFSE/GCE were characterized by scanning electron microscopy (SEM) as shown in Fig.1. Seen from Fig.1A, the PFSE-modified PtNPs are chain-like clusters on the surface of the electrode. It can be speculated that ionic sulfonates clustered and well accommodated those electron deficient platinum nanoparticles due to the anionic and hydrophilic nature of these sulfonates and the hydrophobicity of the PFSE backbone. As shown in Fig.1B, platinum nanoparticles were uniformly adsorbed on the surface of carbon nanotubes. Since the acidified nanotubes contain hydroxyl- and carboxyl-groups, the negatively charged surface facilitates the uniform adsorption of platinum nanoparticles and prevents the aggregation of platinum nanoparticles, and thereby resulting good dispersibility and stability of these PtNPs. Such structure increases the specific area of the modified electrode sensing interface and facilitates the adsorption and bonding of SAL molecules on the electrode surface, thereby enhancing the electrochemical response signal.

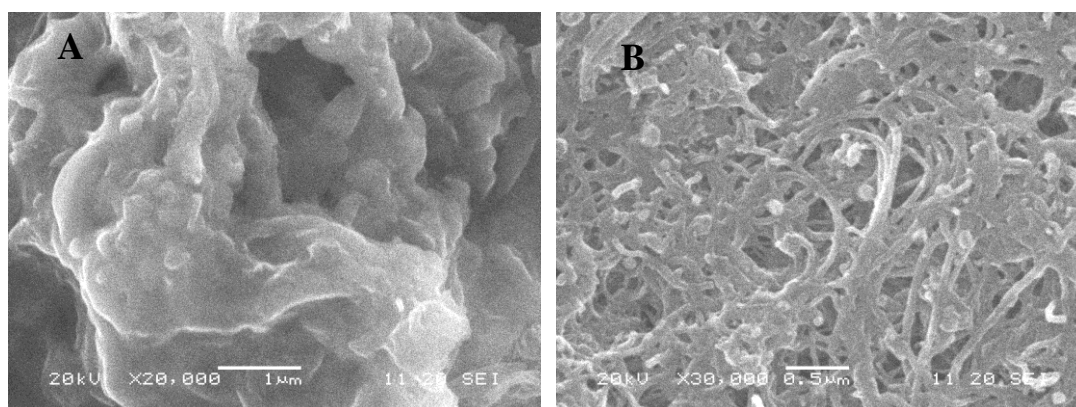


**Figure 1.** SEM images of PtNPs-PFSE/GCE (A) and PtNPs/MWCNTs-PFSE/GCE (B).

The sensor interface was also characterized through electrochemical studies. The cyclic voltammetry characteristics of bare GCE, MWCNTs-PFSE/GCE, PtNPs/GCE, and PtNPs/MWCNTs-PFSE/GCE in 0.1 mol/L KCl solution containing 1.0 mmol/L  $[\text{Fe}(\text{CN})_6]^{4-/3-}$  were investigated (Fig.2A). It is found that the oxidation peak current values of the above electrodes are sequentially enhanced and that of PtNPs/MWCNTs-PFSE/GCE is greater than or equal to the sum of those of MWCNTs-

PFSE/GCE and PtNPs/GCE. The oxidation peak potential of the modified electrode shifts positively compared to the bare GCE, indicating that PtNPs/MWCNTs-PFSE has synergistic electrocatalytic oxidation effect, promoting the electron transfer rate while the single component ones don't.

The effect of different loadings of platinum nanoparticles on carbon nanotubes (4.26%, 8.67%, 10.5%, 18.6%, and 28.7%, respectively) on oxidation peak current of modified electrode was investigated. The electrochemical activity of the modified electrode turned to be the strongest at the loading of 10.5%, which was regarded as the optimum for PtNPs on MWCNTs. At the same time, the actual electrode areas of PtNPs/GCE, MWCNTs-PFSE/GCE, and PtNPs/MWCNTs-PFSE/GCE were calculated as 0.098 cm<sup>2</sup>, 0.112 cm<sup>2</sup>, and 0.215 cm<sup>2</sup>, respectively, according to the Cottrell equation in chronoamperometry [54], indicating their significant increase, which were greater than or equal to the sum of those of MWCNTs-PFSE/GCE and PtNPs/GCE. Such synergistic effect is definitely conducive to electrocatalytic oxidation of the target.

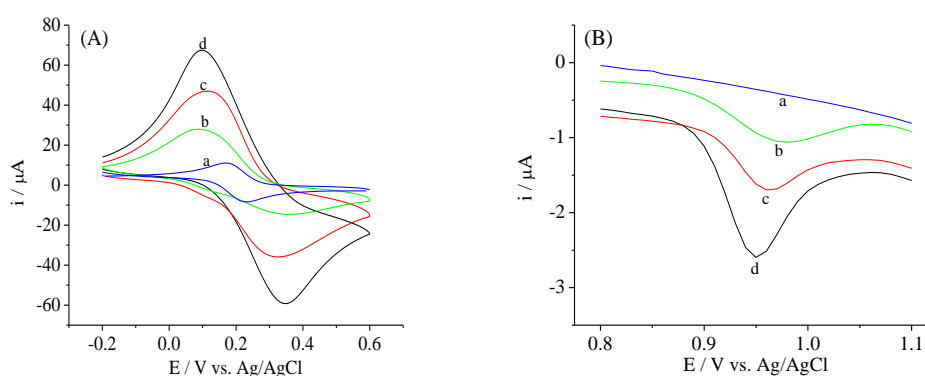


**Figure 2.** (A) Cyclic voltammograms of bare GCE (a), MWCNTs-PFSE/GCE (b), PtNPs/GCE (c), and PtNPs/MWCNTs-PFSE/GCE (d) in 0.1 mol/L KCl solution containing 1.0 mmol/L  $[\text{Fe}(\text{CN})_6]^{4-}/^{3-}$ . (B) Differential pulse voltammetric curves of bare GCE (a), MWCNTs-PFSE/GCE (b), PtNPs/GCE (c) and PtNPs/MWCNTs-PFSE/GCE (d) in PBS (0.1 mol/L, pH=2.5) containing  $6.0 \times 10^{-7}$  mol/L SAL. Scan rate: 60 mV/s.

### 3.2 Differential Pulse Voltammetric Characteristic of Salbutamol on Modified Electrodes

Differential pulse voltammetry (DPV) tests of bare GCE, MWCNTs-PFSE/GCE, PtNPs/GCE, and PtNPs/MWCNTs-PFSE/GCE were performed in 0.1 mol/L PBS (pH=2.5) solution containing  $6.0 \times 10^{-7}$  mol/L salbutamol (SAL), respectively, as shown in Figure 2B. It can be seen that the bare GCE has almost no response to SAL (curve a), MWCNTs-PFSE/GCE presents a relatively distinct oxidation peak at 0.98 V (curve b), the one for PtNPs/GCE appears at 0.96 V with slightly increased current (curve c), while the response current of the modified electrode of PtNPs/MWCNTs-PFSE/GCE to SAL is significantly enhanced (curve d), and the catalytic oxidation peak potential of it to salbutamol is significant negatively shifted compared to that of PtNPs/GCE and MWCNTs-PFSE/GCE electrodes, indicating that the acidified MWCNTs-PFSE composites loaded with PtNPs can dramatically enhance the electrocatalytic oxidation effect of SAL, and the electrocatalytic performance

of such nanocomposite material is better than that of single component modified electrode. This may be attributed to the compact spatial structure between platinum nanoparticles and acidified multi-walled carbon nanotubes which increase the specific surface area of nanocomposites' interface, and synergistically enhance the electrochemical activity of catalytic oxidation of salbutamol.

### 3.3 Cyclic Voltammetric Characteristic of Salbutamol on Modified Electrode

The electrochemical behavior of SAL on PtNPs/MWCNTs-PFSE/GCE has been investigated by cyclic voltammetry. Figure 3A illustrates the cyclic voltammograms of the modified electrode in  $8.0 \times 10^{-7}$  mol/L SAL solution at different scan rates. The results show that a single oxidation peak appears at each cycle during the scan rate of from 10 mV/s to 70 mV/s, and the oxidation peak potential reveals a positive shift with increased scan rates, indicating irreversible process. Meanwhile the peak potential values and the logarithm of the scan rates shows a good linear relationship (Fig. 3B). The linear regression equation can be expressed as  $E_{pa} = 0.746 + 0.092 \lg v$  ( $r = 0.9979$ ). According to Laviron theory [55], for an irreversible adsorption-controlled process, the relationship between  $E_{pa}$  and  $\lg v$  can be determined by the equation below:

$$E_{pa} = E^0 + \frac{2.303RT}{\alpha nF} \lg \frac{RTk^0}{\alpha nF} + \frac{2.303RT}{\alpha nF} \lg v \quad (1)$$

Where  $E^0$  refers to the potential,  $T$  is temperature,  $\alpha$  represents the electron transfer coefficient,  $n$  is the number of transferred electrons,  $k^0$  is the standard heterogeneous electron transfer rate constant, and  $F$  is the Faraday constant. The value of  $\alpha n$  is calculated to be 0.64 from the equation (1). Being an irreversible system, the electron transfer is always a slow process with its value of  $\alpha$  close to 0.5, therefore,  $n$  is calculated to be 1.28, approximately equal 1, indicating the oxidation process of SAL on the modified electrode involves one electron's transfer.

It can seen from Figure 3C that the oxidation peak current of the modified electrode to SAL increases linearly with the increase of the scan rate. The linear regression equation can be expressed as  $i_{pa} (\mu A) = 0.714 + 0.0250v$  ( $V \cdot s^{-1}$ ),  $r = 0.9983$ , indicating that the oxidation of SAL on the modified electrode is an adsorption-desorption process. Therefore, the value of peak current is related to the concentration of the electrode surface active substance and can be determined by the following equation [56]:

$$I_p = \frac{n^2 F^2 A \Gamma v}{4RT} \quad (2)$$

Where  $n$  represents the number of electrons involved in the reaction ( $n=1$ ),  $A$  refers to the actual area of the electrode ( $cm^2$ ),  $I_p$  is the current response value,  $\Gamma$  represents the density of the surface coverage ( $mol \cdot cm^{-2}$ ),  $v$  is scanning rate, and  $F$  is the Faraday constant. According to the relationship between the oxidation peak current of SAL and the scan rate (Fig. 3C), the coverage "density" of PtNPs/MWCNTs-PFSE composites on the electrode surface can be calculated to be  $2.84 \times 10^{-10} mol \cdot cm^{-2}$ .

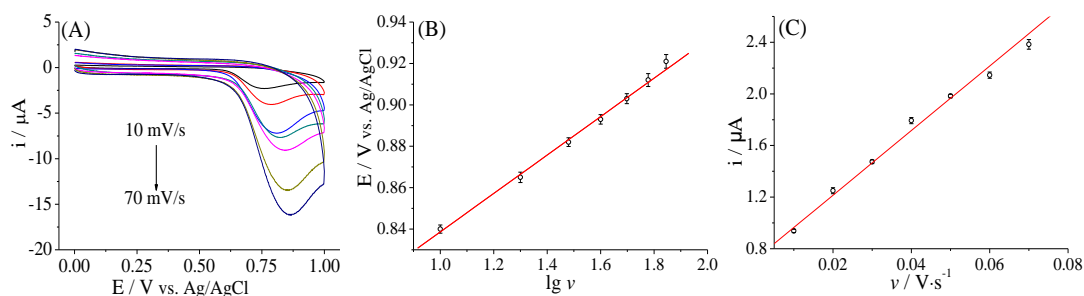


**Figure 3.** Cyclic voltammograms of PtNPs/MWCNTs-PFSE/GCE in PBS (0.01 mol/L, pH=2.5) containing  $8.0 \times 10^{-7}$  mol/L SAL at various scan rates (A), corresponding plots of oxidation peak potential vs.  $\lg v$  (B), and corresponding plots of oxidation peak current vs. scan rate (C).

### 3.4 Effect of pH on Electrochemical Reaction of Salbutamol

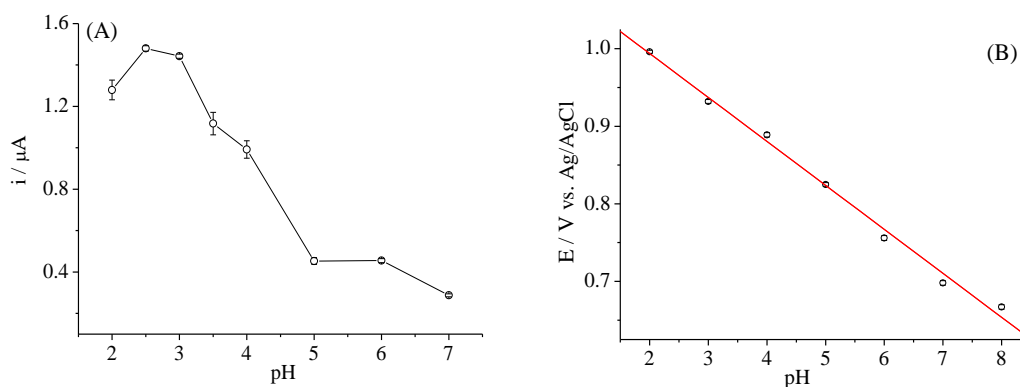


**Figure 4.** Effects of pH on oxidation peak current (A) and the oxidation peak potential (B) of  $5.0 \times 10^{-7}$  mol/L SAL.

pH directly affects the electrochemical behavior of salbutamol on PtNPs/MWCNTs-PFSE/GCE. The influence of pH on oxidation peak current and oxidation peak potential of salbutamol ( $5.0 \times 10^{-7}$  mol/L) in PBS buffer (0.01 mol/L) with pH value in range of 2.0 to 9.0 is shown in Fig. 4A. With reducing pH value from 7.0 to 2.5, the oxidation peak current of SAL gradually increased to its maximum at pH of 2.5, and decreased with further decreased pH. Therefore, pH 2.5 of PBS buffer system was chosen as optimum for the detection of SAL. It can be seen from Fig. 4B that the oxidation peak potential of SAL is negatively shifted with the increased pH values, a linear relationship between oxidation peak potential and pH can be fitted as  $E = 1.107 - 0.056\text{pH}$ ,  $r = 0.9988$ , indicating that it is proton transfer mechanism in the reaction of SAL on the modified electrode with a slope of 0.056. According to the equation of  $E_p = E_0 - 0.059 (m/n) \text{pH}$  ( $m$  is the number of protons transferred during the reaction and  $n$  is the number of electrons transferred during the reaction),  $m/n$  can be calculated to be 0.949, therefore  $m$  is approximately equal to  $n$ . So the oxidation process of SAL on the interface of PtNPs/MWCNTs-PFSE composites is a process which the proton number is equal to that of the number of transferred electron.



### 3.5 Oxidation Mechanism of Salbutamol on Modified Electrode

Based on the above-mentioned electrochemical response characteristics, the proposed oxidation mechanism for salbutamol on PtNPs/MWCNTs-PFSE/GCE was illustrated in Fig.5. A nanocomposite with stable performance and strong electrical activity were prepared by loading the platinum nanoparticles on the surface of multi-walled carbon nanotubes through liquid phase reduction method.

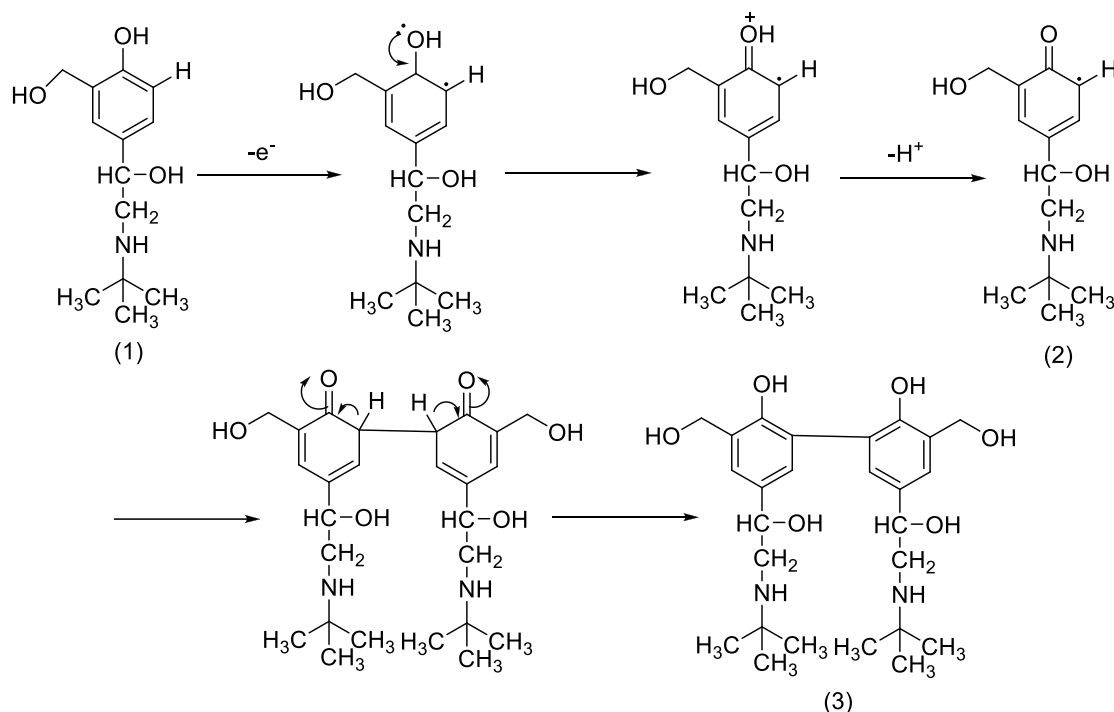


**Figure 5.** Proposed oxidation mechanism of SAL at PtNPs/MWCNTs-PFSE/GCE.

The acidified multi-walled carbon nanotubes functionalized by platinum nanoparticles have strong adsorption capacity and large specific surface area, which can provide more active sites for the oxidation of SAL and promote the catalytic oxidation of SAL on the electrode surface. Since the ion polymer of perfluorinated sulfonic resin (PFSE) exists mesh structure and the precious metal nanoparticles have high conductivity, then the acidified carbon nanotubes functionalized by platinum nanoparticles at the ion polymer matrix will further enhance the electric conductivity of sensing interface. Therefore, the synergistic effect of platinum nanoparticles and multi-walled carbon nanotubes effectively promotes the electron transfer on the metal-carbon nano-polymer interface so that the PtNPs/MWCNTs-PFSE nanocomposites exhibit excellent electrocatalytic oxidation properties.

It is known from the molecular structure of salbutamol that the most likely oxidized site is phenolic hydroxyl group. Combined with the electrochemical behavior of SAL on PtNPs/MWCNTs-PFSE/GCE, the oxidation mechanism of SAL on the modified electrode can be explained as follows: SAL molecules (1) lost one electron and one proton to form a free radical, which can resonate to form intermediate (2), and then transformed a SAL dimer (3) with a C-C bond by combination of two moieties of intermediate (2). This process is an irreversible oxidation reaction, which has been confirmed by CV behavior, as shown in Figure 3A.

### 3.6 Effect of Potential and Time with Enrichment

The effect of potential and time with enrichment on SAL detection of modified electrode was investigated. With the enrichment potential changing from -0.5 V to -0.2 V, the oxidation peak current of SAL on PtNPs/MWCNTs-PFSE/GCE did not change significantly, indicating that the enrichment potential does not affect the voltammetric behavior of the electrode. It was found that the oxidation peak current of SAL increased with improved enrichment time from 0 to 120 s. While exceeding 120s, the oxidation peak current reached its maximum and then remained basically stable, with a saturation equilibrium state that the enrichment of SAL on the surface of electrode reached. Therefore, the optimum enrichment time of 120 s was chosen for the detection of SAL.

### 3.7 Quantitative Detection of Salbutamol

Under the optimum experimental conditions, different concentrations of SAL solution (0,  $5.0 \times 10^{-8}$ ,  $1.0 \times 10^{-7}$ ,  $2.0 \times 10^{-7}$ ,  $5.0 \times 10^{-7}$ ,  $1.0 \times 10^{-6}$ ,  $1.5 \times 10^{-6}$ , and  $2.0 \times 10^{-6}$  mol/L) were detected using PtNPs/MWCNTs-PFSE/GCE, as shown in Fig.6.

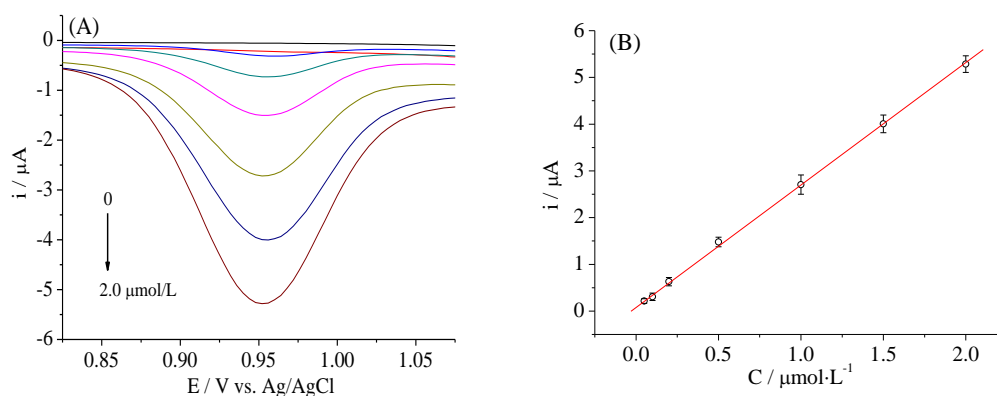


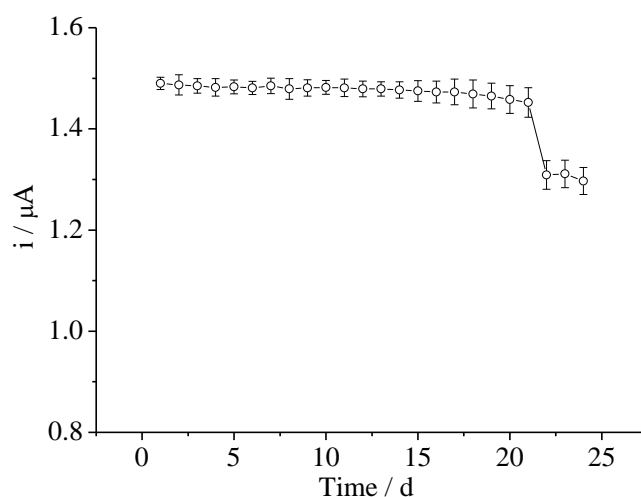
**Figure 6.** Typical DPV curves of peak currents versus logarithm of different concentrations of SAL (A) and the calibration curve (B). The concentration of SAL is 0,  $5.0 \times 10^{-8}$ ,  $1.0 \times 10^{-7}$ ,  $2.0 \times 10^{-7}$ ,  $5.0 \times 10^{-7}$ ,  $1.0 \times 10^{-6}$ ,  $1.5 \times 10^{-6}$ , and  $2.0 \times 10^{-6}$  mol/L, respectively. Scan rate: 60 mV/s.

The oxidation peak current of SAL on the modified electrode increases linearly with increased SAL concentration in the range of  $5.0 \times 10^{-8}$  to  $2.0 \times 10^{-6}$  mol/L, with its linear regression equation as  $i_p(\mu A) = 2.62C(\mu mol/L) + 0.0876$ ,  $r = 0.9992$ . The detection limit is calculated to be  $1.4 \times 10^{-8}$  mol/L from the signal-to-noise characteristics of these data ( $S/N=3$ ), which is better than that of MWCNTs alone modified electrode [28], indicating that the modified electrode has good electrocatalytic response performance to SAL.

**Table 1.** Comparison of various nanomaterial based sensors for SAL detection

| No. | Modified electrode                 | Analyte                   | Linear range ( $\mu\text{mol/L}$ ) | Detection limit ( $\mu\text{mol/L}$ ) | Reference |
|-----|------------------------------------|---------------------------|------------------------------------|---------------------------------------|-----------|
| 1   | Chitosan/MWCNT/GCE                 | Salbutamol                | 0.5-40                             | 0.086                                 | [28]      |
| 2   | Hybrid CNT/Nafion/GCE              | Salbutamol<br>Ractopamine | 0.1-33.3<br>0.05-33.1              | 0.1<br>0.05                           | [35]      |
| 3   | GP/PEDOT:PSS/SPCE                  | Salbutamol                | 5.0 - 550                          | 1.25                                  | [57]      |
| 4   | PASA/GCE                           | Salbutamol                | 2.0-1000                           | 0.65                                  | [58]      |
| 5   | Fullerene-C60/GCE                  | Salbutamol                | 0.418-8.36                         | 0.167                                 | [59]      |
| 6   | Poly taurine/ZrO <sub>2</sub> /GCE | Salbutamol<br>Ractopamine | 5-220<br>1-28                      | 0.02<br>0.15                          | [60]      |
| 7   | GN-Nafion/GCE                      | Salbutamol                | 0.4-30                             | 0.11                                  | [61]      |
| 7   | PtNPs/MWCNTs-PFSE/GCE              | Salbutamol                | 0.050-2.0                          | 0.014                                 | This work |

**Note:** GP/PEDOT:PSS/SPCE represents graphene-poly(3,4-ethylenedioxythiophene):poly (styrene-sulfonate) modified on screen printed carbon electrode. PASA represents poly(aminosulfonic acid).

**Figure 7.** Stability of PtNPs/MWCNTs-PFSE/GCE for continuous detection of  $5.0 \times 10^{-7}$  mol/L SAL.

It can be seen that the electrocatalytic oxidation activity of the metal-carbon nano-polymer composite modified electrode, PtNPs/MWCNTs-PFSE/GCE, is better than that of single material component like MWCNTs [28]. In addition, this method was compared with other reported electrode methods as shown in Table 1. It means the PtNPs/MWCNTs-PFSE/GCE modified electrode has wide linear detection range and low detection limit for SAL, which is better than those of either carbon-nano composite [28, 35, 57-59, 61] or metal oxide-carbon nano-polymer composite [60] modified electrodes reported in the literatures.

### 3.8 Stability

The stability of a sensor is an important performance index for analytical detection applications. The SAL sample of  $5.0 \times 10^{-7}$  mol/L was continuously examined by PtNPs/MWCNTs-PFSE/GCE as a function of time. The differential pulse response signal of the sample on the modified electrode was measured once a day (as shown in Figure 7). The current response value of the modified electrode to SAL was kept almost unchanged within 21d, with an average of the current response value of  $(1.48 \pm 0.09) \times 10^{-6}$  A ( $n=21$ ), that the corresponding relative standard deviation (RSD) was 0.62%. The peak current decreased to 87.9% of the initial response current at 21 d, indicating that the modified electrode has good stability in 21 days and its service life is at least 3 weeks.

### 3.9 Reproducibility and Repeatability

Under the optimum experimental conditions, the DPV response signals of SAL samples with two concentrations of  $3.0 \times 10^{-7}$  mol/L and  $1.0 \times 10^{-6}$  mol/L, respectively, were examined under the same conditions by seven modified electrodes prepared in the same batch. It is found that their relative standard deviations of the two concentrations of SAL samples are 2.6% and 5.1%, respectively, proving good reproducibility. As for the same modified electrode, the relative standard deviations for seven times detection in above two concentrations of SAL samples are calculated to be 1.4% and 4.2%, respectively, indicating that the repeatability of the sensor for the detection of SAL is also excellent.

### 3.10 Interference Detection

As shown in Fig.8, the interference of common cations and common molecules *in vivo* to SAL detection on PtNPs/MWCNTs-PFSE/GCE was investigated under the optimum experimental conditions. It is found that 500-fold concentrations of  $\text{Ba}^{2+}$ ,  $\text{Zn}^{2+}$ ,  $\text{Al}^{3+}$ , and 100-fold concentrations of uric acid, ascorbic acid, glucose, urea, glycine, L-arginine, L-leucine, L-cysteine, and L-tyrosine had almost no influence on the detection of  $5.0 \times 10^{-7}$  mol/L SAL, within the relative error of  $\pm 5\%$ . And the same concentration of clenbuterol had a relatively small effect on the detection of SAL, causing a increase of response current by about 7.9%, while the same concentration of ractopamine did not affect the detection of SAL at all.

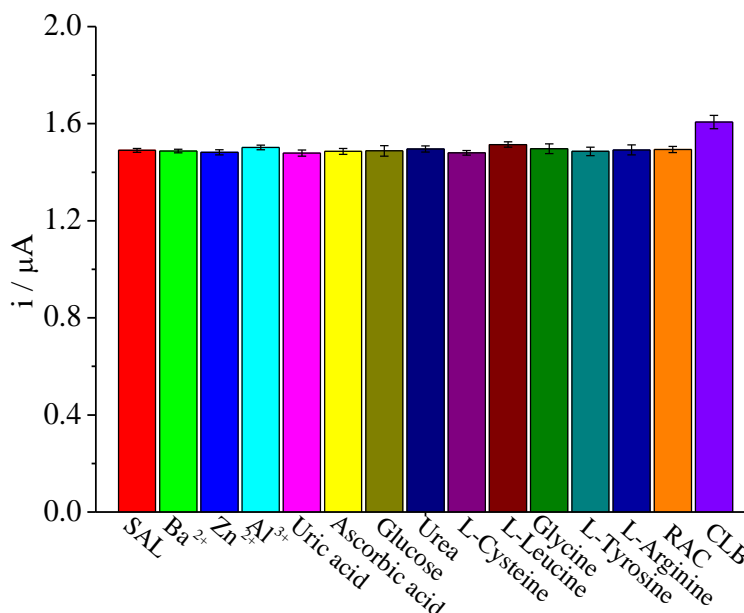


**Figure 8.** Effect of interfering substance on the modified electrode with their concentration of  $5.0 \times 10^{-7}$  mol/L for SAL,  $2.5 \times 10^{-4}$  mol/L for  $Ba^{2+}$ ,  $Zn^{2+}$ , and  $Al^{3+}$ ,  $5.0 \times 10^{-5}$  mol/L for uric acid, ascorbic acid, glucose, urea, L-leucine, L-cysteine, L-alanine, and L-tyrosine,  $5.0 \times 10^{-7}$  mol/L for CLB and RAC.

### 3.11 Analytical Application in pork meat and pork liver

As practical applications, the contents of SAL in six samples of pork meat and pork liver from ternary hybrid piglets were examined by PtNPs/MWCNTs-PFSE modified electrode. The results were shown in Table 2. As seen from Table 2, the composites modified electrode can be applied to the detection of SAL in actual samples of pork meat and pork liver with a recovery rate of 95.4 to 104.3% and 97.9 to 103.8%, which shows promising application prospect on food safety detection.

**Table 2.** Determination of SAL in pork meat and pork liver samples with application of PtNPs/MWCNTs-PFSE/GCE.

| Real Sample |   | Spiked<br>( $\mu g/kg$ ) | Measured <sup>a</sup><br>( $\mu g/kg$ ) | Recovery<br>(%) |
|-------------|---|--------------------------|---|-----------------|
| Pork meat   | A | 2.50                     | 2.58 ( $\pm 0.18$ )                     | 103.2           |
|             | B | 5.00                     | 4.77 ( $\pm 0.22$ )                     | 95.4            |
|             | C | 10.00                    | 10.43 ( $\pm 0.46$ )                    | 104.3           |
|             | D | 15.00                    | 15.57 ( $\pm 0.35$ )                    | 103.8           |
| Pork liver  | E | 20.00                    | 19.81 ( $\pm 0.27$ )                    | 99.1            |
|             | F | 25.00                    | 24.47 ( $\pm 0.49$ )                    | 97.9            |

**Note:** <sup>a</sup> The data in the parenthesis are the standard deviations ( $n=3$ ).

#### 4. CONCLUSION

In this work, a novel metal-carbon nano-polymer matrix modified glassy carbon electrode, named as PtNPs/MWCNTs-PFSE/GCE was successfully prepared. With the mesh structure of the ion polymer of perfluorinated sulfonic resin as the matrix, the synergistic effect of platinum nanoparticles and multi-walled carbon nanotubes effectively promotes the electron transfer on the metal-carbon nano-polymer interface. The electrode exhibited significantly electrocatalytic oxidation activity to salbutamol (SAL). The oxidation mechanism has been explored that the phenolic hydroxyl group of SAL (1) is oxidized involving one proton and one electron with its formation of a free radical, forming intermediate (2) via resonance, and then transforms to a SAL dimer (3) with a C-C bond formation via re-combination of intermediate (2). Under the optimum experimental condition, the composite modified electrode shows good electrochemical response to SAL in the range from  $5.0 \times 10^{-8}$  mol/L to  $2.0 \times 10^{-6}$  mol/L with its detection limit of  $1.4 \times 10^{-8}$  mol/L. The modified electrode exhibited good selectivity, excellent reproducibility and long useful stability, which was successfully applied to detection of SAL in pork meat and pork liver samples with a recovery rate from 95.4% to 104.3%, indicating its important practical applications in food safety control.

#### ACKNOWLEDGEMENTS

This work was financially supported by the projects of National Natural Science Foundation of China (No. 21545010), Natural Science Foundation of Hunan Province of China (No. 2020JJ4599), and Key Project of Hunan Provincial Education Department of China (No. 17A002).

#### References

1. G.R. Kelman, K.N. Palmer and M.R. Cross, *Nature*, 221 (1969) 1251.
2. M. Patel, J. Pilcher, A. Pritchard, K. Perrin, J. Travers, D. Shaw, S. Holt, M. Harwood, P. Black, M. Weatherall and R. Beasley, *Lancet Respir. Med.*, 1 (2013) 32.
3. K.J. Reszka, D.W. McGraw and B.E. Britigan, *Chem. Res. Toxicol.*, 22 (2014) 1137.
4. C. Frugier, F. Graham, K. Samaan, L. Paradis, A. Des Roches and P. Bégin, *J. Aller. Clin. Immun.: In Practice*, 9 (2021) 3130.
5. A. Samir, H.M. Lotfy, H. Salem and M. Abdelkawy, *Spectrochim. Acta A*, 128 (2014) 127.
6. Q. Zhang, Y. Ni and S. Kokot, *J. Agric. Food Chem.*, 61 (2013) 7730.
7. M. Li, Y.Y. Zhang, Y.L. Xue, X. Hong, Y. Cui, Z.J. Liu and D.L. Du, *Food Control.*, 73 (2017) 1039.
8. Y.M. Koh, M.I. Saleh and S.C. Tan, *J. Chromatogr. A.*, 987 (2003) 257.
9. K.P. Yan, H.Q. Zhang, W.L. Hui, H.L. Zhu, X.B. Li, F.Y. Zhong, X.E. Tong and C. Chen, *J. Food. Drug. Anal.*, 24 (2016) 277.
10. M.W.F. Nielen, J.J. Lasaroms, M.L. Essers, J.E. Oosterink, T. Meijer, M.B. Sanders and T. Zuidema, *Anal. Bioanal. Chem.*, 391 (2008) 199.
11. Z. Guo, Y. Chen, X. Ding, C. Huang and L. Miao, *Biomed. Chromatogr. BMC.*, 30 (2016) 1789.
12. S.H. Chan, W. Lee, M.Z. Asmawi and S.C. Tan, *J. Chromatogr. B.*, 1025 (2016) 83.
13. L. Wang, Y.Q. Li, Y.K. Zhou and Y. Yang, *Chromatographia*, 71 (2010) 737.
14. G. Forsdahl and G. Gmeiner, *J. Sep. Sci.*, 27 (2015) 110.
15. M.K. Parr, G. Opfermann and W. Schanzer, *Bioanalysis*, 1 (2009) 437.

16. W. Xu, X.L. Chen, X.L. Huang, W.C. Yang, C.M. Liu, W.H. Lai, H.Y. Xu and Y.H. Xiong, *Talanta*, 114 (2013) 160.
17. T.T. Dong, Q.H. Tang, M. Chen and J.G. Li, *J. Electrochem. Soc.*, 163 (2016) B62.
18. X. Zhang, Y.X. Chu, H. Yang, K. Zhao, J.G. Li, H.J. Du, P. She and A.P. Deng, *Food. Anal. Methods*, 9(2016) 1.
19. K.J. Zhu, L. Zhou, L. Wu, S.F. Feng, H.Y. Hu, J.L. He, Y.M. He, Z.M. Feng, Y.L. Yin, D. Yu and Z. Cao, *Chinese J. Chem.*, 39 (2021) 2755.
20. Z. Cao, W.-F. Li, C. Liu, Y.-Y. Peng, Y. Huang and Z.-L. Xiao, *Chinese J. Anal. Chem.*, 47 (2019) 229.
21. J. Yang, Y.-Y. Zhang, C. Liu, J.-X. Li, Z.-L. Xiao, D. Li, L. Zhang and Z. Cao, *Chem. J. Chinese Universities*, 39 (2018) 2386.
22. Y.Q. Li, Q. Zhu, Z.L. Xiao, C.Z. Lü, Z.M. Feng, Y.L. Yin and Z. Cao, *Chem. J. Chinese Universities*, 39 (2018) 636.
23. C.Z. Lv, D. Chen, Z. Cao, F. Liu, X.M. Cao, J.L. He and W.Y. Zhao, *Int. J. Electrochem. Sci.*, 11 (2016) 10107.
24. Y. Wang, D. Li, J.F. Kang, S.Y. Guan and D.X. Wu, *Int. J. Electrochem. Sci.*, 14 (2019) 5448.
25. L. Wu, Z. Cao, T. Song, C. Song, J. Xie, J. He and Z. Xiao, *Chinese J. Anal. Chem.*, 42 (2014) 1656.
26. M.-L. Zhang, Z. Cao, J.-L. He, L. Xue, Y. Zhou, S. Long, T. Deng and L. Zhang, *Food Addit. Contamin. A*, 29 (2012) 1938.
27. G. Li, Y. Wang, Y. Cao, Z. Xiao, Y. Huang, Z. Feng, Y. Yin and Z. Cao, *Chem. J. Chinese Universities*, 38 (2017) 1953.
28. Z. Cao, Y.T. Zhao, Y.M. Dai, S. Long, X.C. Guo and R.H. Yang, *Sensor Lett.*, 9 (2011) 1985.
29. T. Alizadeh and L.A. Fard, *Anal. Chim. Acta.*, 769 (2013) 100.
30. Y.B. Qi, Y. Liu and Q.J. Song, *Chinese J. Anal. Chem.*, 39 (2011) 1053.
31. Z.T. Cui, Y.Y. Cai, D. Wu, H.Q. Yu, Y. Li, K.X. Mao, H. Wang, H.X. Fan and Q. Wei, *Electrochim. Acta.*, 69 (2012) 79.
32. D. Boyd, J.R.B. Rodriguez, A.J. Ordieres, P.T. Blanco and M.R. Smyth, *Analyst*, 119 (1994) 1979.
33. R.N. Goyal, M. Oyama and S.P. Singh, *J. Electroanal. Chem.* 611 (2007) 140.
34. C. Karuwan, A. Wisitsoraat, T. Maturos, D. Phokharatkul, A. Sappat, K. Jaruwongrunsee, T. Lomas and A. Tuantranont, *Talanta*, 79 (2009) 995.
35. K.C. Lin, C.P. Hong and S.M. Chen, *Sens. Actuators B*, 177 (2013) 428.
36. A. Corma, H. Garcia and A. Leyva, *J. Mol. Catal. A-Chem.*, 230 (2005) 97.
37. D. Chen, Z. Cao, F. Liu, L. Wu, Y. Xun, J. He and Z. Xiao, *Chinese J. Anal. Chem.*, 44 (2016) 1593.
38. Z. Cao, Q. Zhu, Y. W. Lin and W. M. He, *Chinese Chem. Lett.*, 30 (2019) 2132.
39. E. Mohammadi, Z. Hajilou and B. Movassagh, *Helv. Chim. Acta.*, 99 (2016) 747.
40. O.A. Cano, C.A.R. Gonzalez, J.F.H. Paz, P.A. Madrid, P.E.G. Casillas, A.L.M. Hernandez and C.A.M. Perez, *Catal. Today.*, 282 (2017) 168.
41. Z.D. Wei, C. Yan, Y. Tan, L. Li, C.X. Sun, Z.G. Shao, P.K. Shen and H.W. Dong, *J. Phys. Chem.*, 112 (2008) 2671.
42. Z.Z. Zhu, J.L. Wang and H.S. Zhou, *Electrochim. Acta.*, 55 (2010) 8517.
43. M. Huang, J. Zhang, C. Wu and L. Guan, *ACS Appl. Mater. Interfaces*, 9 (2017) 26921.
44. Y. Xun, Z. Cao, T. Song, C.Z. Lü, F. Liu, J. He and R. Yang, *Chem. J. Chinese Universities*, 37 (2016) 835.
45. C.Z. Lv, Y. Xun, Z. Cao, J.L. Xie, D. Li, G. Liu, L. Yu, Z.M. Feng, Y.L. Yin and S.Z. Tan, *Food Anal. Methods*, 10 (2017) 2252.
46. W.W. Li, R.Z. Ouyang, W.Y. Zhang, S. Zhou, Y. Yang and Y.J. Ji, *Electrochim. Acta*, 188 (2016) 197.
47. L. Liu, Y. You, K. Zhou, B. Guo, Z. Cao, Y. Zhao and H. C. Wu, *Angew. Chem. Int. Ed.*, 58 (2019)

- 14929.
48. Q. Zhu, C. Liu, L. Zhou, L. Wu, K.J. Bian, J.L. Zeng, J.X. Wang, Z.M. Feng, Y.L. Yin and Z. Cao, *Biosens. Bioelectron.*, 140 (2019) 111356.
49. Y. Sheng, Y. You, Z. Cao, L. Liu and H.-C. Wu, *Analyst*, 143 (2018) 2411.
50. Y. You, K. Zhou, B. Guo, Q. Liu, Z. Cao, L. Liu and H.-C. Wu, *ACS Sens.*, 4 (2019) 774.
51. S. Long, Y.F. Tian, Z. Cao, J.L. He and D.M. Luo, *Sens. Actuators: B. Chem.*, 166-167 (2012) 223.
52. M.-L. Zhang, D.-K. Huang, Z. Cao, Y.-Q. Liu, J.-L. He, J.-F. Xiong, Z.-M. Feng and Y.-L. Yin, *LWT-Food Sci. Tech.*, 64 (2015) 663.
53. Y.Y. Peng, Y. Wang, X.Y. Yu, J.L. Zeng, Z.L. Xiao and Z. Cao, *Chem. J. Chinese Universities*, 41 (2020) 268.
54. X.J. Huang, H.S. Im, O. Yarimaga, J.H. Kim and D.H. Lee, *J. Phys. Chem. B.*, 110 (2006) 21850.
55. E. Laviron, *Interfacial Electrochem, J. Electroanal. Chem.*, 101 (1979) 19.
56. J. Wang, *Analy Electrochemistry*, Translated by Y.C. Zhu and L. Zhang, *Chemical Industry Press, Beijing*, 2008, pp.29.
57. C. Karuwan, C. Sriprachuabwong, A. Wisitsoraat, D. Phokharatkul, P. Sritongkham, A. Tuantranont, *Sens. Actuators B*, 177 (2012) 549.
58. L.J. Li, L.B. Yu, H. Cheng, Q.F. Chen, F.M. Wu, T. Chen, X.Y. Zhu, H.X. Kong and J.L. Wu, *Anal. Lett.*, 40 (2007) 3290.
59. R.N. Goyal, D. Kaur, S.P. Singh and A.K. Pandey, *Talanta*, 75 (2008) 63.
60. M. Rajkumar, Y.S. Li and S.M. Chen, *Colloid. Surface. B.*, 110 (2013) 242.
61. Y.L. Zhou, H.Q. Zhang, Z. Chang, B.X. Ye and M.T. Xu, *Int. J. Electrochem. Sci.*, 11 (2016) 5154.